A GENERAL THEORETICAL CONSTRAINT AT M = 1 FOR INTRUSIVE PROBES and SOME TRANSONIC CALIBRATIONS OF SIMPLE STATIC-PRESSURE AND FLOW-DIRECTION PROBES

P.E.Hancock
University of Surrey
(formerly, Central Electricity Research Laboratories,
Leatherhead, U.K.)

1. INTRODUCTION

Measurements in high-subsonic, transonic and supersonic flows are often made by means of intrusive probes, and considerable attention is given to the calibrations of these probes (eg the 7th Proceedings of this series of meetings). The most difficult regime is the transonic range, especially in internal flows. However, it would appear that the existence of a theoretical constraint at M=1 has been overlooked: the basis of the constraint is given in the texts of Liepmann & Roshko(1966) and Shapiro(1954), and possibly elsewhere, but has not been applied to probe calibrations - at least as far as the open literature available to the author is shows. The contraint applies to any intrusive probe, though not irrespectively of its shape.

The constraint is derived in Section 2 in the context of pressure-sensing probes, although the constraint applies to any probe - e.g. velocity-sensing probe. The principal result is that the sensitivity of any static-pressure probe to static pressure must be zero at M=1. It follows that the sensitivity near M=1 must be low. A further implication is that the insensitivity to the static pressure can disguise an error in a calibration arising from an error in the 'true' static pressure, which is usually not easy to determine in transonic flows. Flow-direction probes on the other hand retain a non-zero sensitivity to flow-direction but the sensitivity is reduced through M=1.

In Sections 4 and 5 some transonic calibrations of simple disk-type static pressure probes and two-hole Conrad flow-direction probes are given, partly to demonstrate the theoretical constraint in the vicinity of M=1. However, they are also included for two other reasons. Firstly, because other features are demonstated which, as far as the presert author is aware, are not mentioned in the literature. Secondly, because the present calibrations were of probes with relatively simple geometries. The calibrations where made in the slightly wet, low-pressure steam in the CERL steam tunnel in the course of other work. Wetness effects were negligible. Details of the probes are given in Figure 1. The Conrad probes were made according to the guidelines given by Chue(1975). Although the yaw probe was to be used as "nulling" device - i.e. rotating it a measured angle for zero pressure difference between the sensing holes - its use in this manner requires a well behaved yaw calibration.

The effects of transverse gradients of Mach number or total pressure, or both, are, it is argued, likely to be large in the transonic range, causing doubt about the accuracy of measurements in non-uniform transonic flows. Streamwise-gradients of Mach number are also likely to cause errors. Shock reflections, blockage effects, etc

in internal flows are not considered here, but are likely to cause further errors, of course.

2 THEORETICAL CONSIDERATIONS AT M = 1

The distance a detached shock stands ahead of a body in a uniform supersonic flow increases indefinitely, and its strength tends to zero, as the Mach number, M, ahead of the shock tends to unity. This is because at Mach numbers very slightly less than unity disturbances must travel in all directions to infinty: if the detached shock strength became zero at a finite distance then there would have to be a discontinuity in flow pattern at M=1. Therefore, at Mach numbers very slightly above unity the shock stands well ahead of the probe and must be very nearly normal to the flow (and, of course, very weak). It follows that the Mach number M^ of the flow downstream of the shock is just subsonic. Thus in the limit, as M (>1) tends to unity, the flow over the probe becomes identical to a subsonic free-stream flow at Mach number M^, which, from the normal-shock relations, is related to M by $M^ = 2 - M$.

Now if M' is the Mach number at an arbitrary point on or near the probe, it follows that

$$\lim_{M\to 1}\left(\frac{dM'}{dM}\right) = 0. \qquad 2.1$$

From the normal-shock relations it is straightforward to show that

$$\lim_{M\to 1}\frac{d}{dM}\left(\frac{p_o^\wedge}{p_o}\right) = 0, \qquad 2.2$$

where p_o and $p_o^\wedge$ are the total pressures upstream and downstream of the shock, respectively. If p' is the pressure at the arbitrary point then, because the flow downstream of the shock is isentropic,

$$\frac{p'}{p_o} = \frac{p_o^\wedge}{p_o}\left(1+\frac{\gamma-1}{2}M'^2\right)^{\frac{-\gamma}{\gamma-1}} . \qquad 2.3$$

Differentiating w.r.t. M gives

$$\frac{d}{dM}\left(\frac{p'}{p_o}\right) = \left(1+\frac{\gamma-1}{2}M'^2\right)^{\frac{-\gamma}{\gamma-1}}\frac{d}{dM}\left(\frac{p_o^\wedge}{p_o}\right) - \gamma M\left(1+\frac{\gamma-1}{2}M'^2\right)^{-1}\frac{p'}{p_o}\frac{dM'}{dM} , \qquad 2.4$$

so that in the limit M=1

$$\lim_{M\to 1}\left(\frac{dp'}{dp_o}\right) = 0 . \qquad 2.5$$

If p is the static pressure upstream of the shock then

$$\frac{d}{dM}\left(\frac{p}{p_o}\right) = \frac{d}{dM}\left(1+\frac{\gamma-1}{2}M'^2\right)^{\frac{-\gamma}{\gamma-1}}$$

$$= \quad - \gamma M \left(1+\frac{\gamma-1}{2} M'^2\right)^{-1}$$

and so

$$\lim_{M\to 1} \frac{d}{dM}\left(\frac{p}{p_o}\right) = -\frac{2\gamma}{\gamma+1} \qquad 2.6$$

Thus, whilst p/p_o changes with M as M passes through unity, at the rate given by equation 2.5, p'/p_o does not. That is, the pressure p' is insensitive to changes in the pressure p as M passes through unity; the sensitivity of any probe - such as a static-pressure probe - to a change in static pressure p (or, equivalently, Mach number) is zero at M=1. It follows that the sensitivity near M=1 must be low.

The disk-probe calibration are presented in the form $p'/p \sim M$. From equations 2.5 and 2.6 the limiting gradient for the ratio becomes

$$\left.\frac{d}{dM}\left(\frac{p'}{p}\right)\right|_{M=1} = \left.\frac{2\gamma}{\gamma+1}\,\frac{p'}{p}\right|_{M=1} \qquad 2.7$$

Hence, at M=1, the gradient of the calibration expressed in terms of p'/p as a function of M is equal to p'/p at M=1 multiplied by the factor $2\gamma/(\gamma+1)$. Moreover, since p'/p must always be positive it follows that the left hand side of equation 2.7 must also always be positive. At low Mach numbers where compressibility effects are small the pressure ceofficient C_p, defined as $C_p = (p'-p)/\gamma p M^2/2$, is very nearly independent of Mach number, whereupon $\partial(p'/p)/\partial M = \gamma M C_p$: the sign of $\partial(p'/p)/\partial M$ depends upon the sign of C_p. Thus, if C_p is negative in this range then $\partial(p'/p)/\partial M$ must change sign somewhere in the higher subsonic Mach number range, whereas this is probably not so if C_p is positive.

If $\Delta p'$ is the difference of two pressures on or near the probe then it follows from equation 2.7 that

$$\left.\frac{d}{dM}\left(\frac{\Delta p'}{p}\right)\right|_{M=1} = \left.\frac{2\gamma}{\gamma+1}\,\frac{\Delta p'}{p}\right|_{M=1}$$

In Section 5 the flow-direction probe calibrations are expressed in terms of a pressure coefficient, C_p, where

$$C_p = \frac{\Delta p}{\gamma p M^2/2}$$

whereupon it follows that

$$\left.\frac{dC_p}{dM}\right|_{M=1} = -\left.\frac{2\gamma}{\gamma+1} C_p\right|_{M=1}, \qquad 2.8$$

and that

$$\frac{d}{dM}\frac{\partial C_p}{\partial \psi}\bigg|_{M=1} = -\frac{2\gamma}{\gamma+1}\frac{\partial C_p}{\partial \psi}\bigg|_{M=1} . \qquad 2.9$$

where ψ is a yaw (or, with ϕ instead of ψ, a pitch) angle. Flow angle are defined in Figure 3.

An inversion function I(M) is defined by equation 4.2 in Section 4. Applying the above arguments leads to the result that

$$\frac{d}{dM}I(M)\bigg|_{M=1} = 0. \qquad 2.10$$

Indeed, if K, say, is any arbitrary non-dimensional calibration coefficient defined purely in terms of pressures on (or near) the probe, or non-dimensionalised by the upstream total pressure then the basic argument implies that $\partial K/\partial M = 0$ at M=1.

From the basic argument it also follows that streamline directions adjacent to and near the probe should be invariant with Mach number in the limit M=1. Thus for example $\partial\psi_o/\partial M$ and $\partial\phi_o/\partial M$, where ψ_o and ϕ_o are defined in Section 5, should be zero at M=1.

3 CALIBRATION FACILITY

The transonic test section, which is shown in Figure 2, has been discussed by Wood(1983), but the main points are briefly repeated here. The test-section Mach number in the range $0.87 < M < 1.2$ was controlled by means of the flaps which allowed the flow to expand through the two porous walls. These walls performed a double function, the other being the elimination of incident shock waves. The test-section static pressure was inferred from wall tappings in one of the non-porous side walls. The probe to be calibrated was supported in a 25.4mm dia plug which was mounted in one of two circular windows, itself mounted in the other side wall. Depending upon the circular window employed the probe pitch could be set at $\phi = 0^o$, $+10^o$ or -10^o - see Figure 3 for definition of angles. The geometrical blockage area imposed by each probe head and body was ~0.52%. Mach numbers less than 0.87 were achieved by either reducing the mass flow or by raising the back pressure, the former reducing the Reynolds number but the latter leaving it roughly constant.

It was not possible to permanently mount a total pressure probe in the test section such that for supersonic flow its shock wave affected neither the probe to be calibrated nor the wall-tapping pressures, and such that it was itself unaffected by the probe to be calibrated. In subsonic dry-gas flows the total pressure can be measured in the settling chamber, but here there was a small loss of total pressure due to fine droplets. At supersonic Mach numbers an additional loss arose from low-intensity weak shock waves (or "shocklets") emanating from the flow over the perforated walls. Therefore, the Pitot-type total-pressure probe was positioned as shown in Figure 2, and moved to the retracted position shown once the total pressure had been measured. The Mach number in this paper is the gas-phase (or 'frozen flow') Mach number, where a value of $\gamma=1.3$ has been used throughout. Wetness levels were 0.02 by mass fraction or less. No adjustments were made to the measured total pressure. The error in Mach number is less than 1%, and the effect on the

calibrations, as determined by some measurements in super-heated steam showed no effect of wetness.

Wall effects arising from solid side walls were not examined in detail. Other probe-calibration work in the same facility had indicated no significant effect, but since no detailed investigation was made in the present work it is not possible to be certain that wall effects were not significant.

Errors in Mach number and pressure arising from systematic measurement errors are listed below

M	0.6	1.2
δM	±0.9%	±0.6%
$\delta p/p$	±0.3%	±0.8%

whilst errors associated with drift in tunnel conditions, etc were within about ±0.5% and ±0.3% in M and p, respectively. The errors at the lower Reynolds number were about twice the above figures.

4 DISK-PROBE CALIBRATIONS

Figure 4 shows the pressure ratio p_d/p as a function of Mach number, M, and pitch, ϕ, for probe DA where p_d is the pressure sensed by disk probe. This figure also includes the theoretical slope given by equation 2.7 plotted through the measured value of $(p_d/p)_{M=1}$. The measured calibration clearly conforms to the theoretical slope in the range $1 \leq M \leq 1.1$, although the high degree of coincidence towards the upper end of this range must be regarded as largely fortuitous. This is because, although the extent, ΔM, over which the linear variation might be approximately correct cannot be determined from the analysis, the basis of the analysis implies the range of approximate validity would be $1-\Delta M \leq M \leq 1+\Delta M$, which is clearly not so in these cases for any significant ΔM (>0.01, say).

Above the linear region two of the curves show fairly sharp peaks and rapid decreases in p_d/p with M. The decrease is to be expected if the behaviour of the probe is to tend to that for an aerodynamically thin body with an attached leading-edge shock.

The broken curve shown in Figure 4 is a curve of constant pressure coefficient, defined by

$$C_p = \frac{p_d - p}{\gamma p M^2/2} \qquad 4.1$$

Some variation of C_p with M is to be expected in this range although the assumption of constant C_p would appear to be reasonable for a moderate range of M. Note, the Prandtl-Glauert similarity law $C_p=C_{po}(1-M^2)^{1/2}$, where C_{po} is the pressure coefficient at M=0, applies to only two-dimensional flow: the finite span precludes this form of similarity law for subsonic irrotational flow about thin three-dimensional bodies.

The inversion function I(M), which assumes a total pressure measurement p_{om}, is shown in Figure 5 and 6 for the (smoothed) calibration data of probe DA (given in Figure 4) and probe DB. I(M) is defined by

$$I(M) = \frac{p_{om}}{p_d} = \frac{(p_{om}/p_o)(p_o/p)}{(p_d/p)} \qquad 4.2$$

where for $M \leq 1$ $p_{om}/p_o = 1$, and for $M > 1$ p_{om}/p_o is given by the relationship for total pressure across a normal shock. As shown in Section 2, equation 2.10, $dI(M)/dM$ is zero at M=1, and the weak dependence of I(M) near M=1 is therefore to be expected. The pitch effect is clearly evident and is large in the range $0.8 \leq M \leq 1.2$. For example, a pitch error of 10^o can give a Mach number error δM of up to $\delta M = 0.2$.

The differences between the calibrations in the two disk probes - Figures 5 & 6 - were probably due to differences in disk profile, which was not finely controlled, and the difference in the probe support. The Reynolds number Re_d in Figure 4 is based on the disk diameter.

5 FLOW-DIRECTION PROBE CALIBRATIONS

5.1 Yaw probes

Figure 7 shows the difference in pressures p' and p" sensed by the two holes of the yaw probe YA as a function of yaw angle and Mach number in terms of the pressure coeficient defined by

$$C_p = \frac{p'' - p'}{\gamma p M^2/2} \qquad 5.1$$

At constant M, Cp is linear with respect to ψ to within $<1^o$ over the range $-15^o \pm \psi \pm +15^o$. Figure 8 shows the Mach number variation of the sensitivity gradient $\partial C_p/\partial \Psi$ and the yaw angle ψ_o at which C_p is zero. The sensitivity below M = 0.85 is evidently closely constant at $\partial C_p/\partial \psi = 0.048$ which is comparable with other two-hole Conrad probes of similar apex angle and tube-diameter ratio. Bryer & Pankhurst (1971) indicate for incompressible flow a sensitivity between 0.043 to 0.050, and quote 0.49 as typical. A decrease in $\partial C_p/\partial \psi$ with Mach number near M=1 is to be expected for the reasons given in Section 2, and the data can be seen to be consistent with the theoretical slope, equation 2.9. Also, the smooth (and in fact only slight) variation of $\partial C_p/\partial \psi$ with M at supersonic Mach numbers is most likely helped by the fact that the apex angle was large enough to have maintained a detached shock. A shock attachment is likely to cause a sudden change in the sensitivity. Comparable results were obtained for probe YB. Departure of ψ_o from zero accounts for asymmetry of the probe and probe-setting angle errors with respect to the flow direction which was assumed to be parallel to the tunnel centre line. The slight variation with Mach number is within the setting error.

Figure 10b shows pressure coefficients based upon the mean tube pressure (p'+p")/2 and the static pressure p, and upon (p'+p")/2 and the measured total pressure, p_{om}. An inversion function similar to that defined by equation 4.2, namely the pressure ratio, $2p_{om}/(p'+p")$, is shown in Figure 10a for the probe aligned with the flow. Clearly, because of the small variation with Mach number, such a probe is considerably less useful than the disk probe for measuring static pressure. Furthermore, compared with p_{om}/p, $2p_{om}/(p'+p")$ did not differ substantially from unity over the given Mach number range, suggesting that this type of probe would not be very accurate as a static pressure probe at lower Mach numbers. This is consistent with the finding of Dudzinski & Krause (1969) for the range $0.3 < M < 0.9$.

5.2 Pitch probes

Figure 9 shows the pitch-probe sensitivity $\partial C_p/\partial\phi$ and the zero-C_p pitch angel, ϕ_o, for probe PB. The results for probe PA were consistent with those for PB. C_p is defined by eqation 5.1 where p' and p" are here the pressures sensed by the inner and outer tubes respectively. $\partial C_p/\partial\phi$ is evidently higher than that for the yaw probes, increasing over nearly the entire subsonic range from a sensitivity at low Mach numbers fairly close to that for the yaw probes. This increase in sensitivity with Mach number would appear to be an effect of the support body since it does not appear in the yaw probe calibrations where the support body is perpendicular to the plane of flow-direction sensitivity, the sensing-head geometries being the same for both probes. Presumably, this effect is related to the pitch-sensitivity of the disk probes. For the simple reason of asymmetry of the pitch probe in the pitch plane C_p at zero pitch would not be zero. Near M=1 the decrease in sensitivity is comparable with the theoretical reduction.

6 FURTHER COMMENTS

Figure11 shows some of the data from the calibration exercises reported at the 7th Symposium for the WP11 probe, together with the theoretical slope at M=1. Although the agreement between the calibrations is apparently better near M=1 and in reasonable if not good agreement with the theoretical slope the aggreement is illusory if the Mach number, M, is obtained from the 'true' static pressure, p, (or vice versa). This can be shown as follows.

If we write

$$\frac{p'}{p} = \frac{p'}{p_o}\left(1+\frac{\gamma-1}{2}M^2\right)^{\frac{-\gamma}{\gamma-1}}$$

and note that p'/p_o is fixed in the present context, the rate of change of p'/p with M is given by

$$\frac{d}{dM}\left(\frac{p'}{p}\right) = \gamma M\left(1+\frac{\gamma-1}{2}M^2\right)^{-1}\frac{p'}{p} \quad ,$$

so that at M=1

$$\left.\frac{d}{dM}\left(\frac{p'}{p}\right)\right|_{M=1} = \left.\frac{2\gamma}{\gamma+1}\frac{p'}{p}\right|_{M=1} .$$

This is the same as the result of equation 2.7 in Section 2. Thus, near M=1 an error in p is such that the plotted values of p'/p and M are displaced in a direction closely coincident with the theoretical result for the true calibration curve at M=1. The same conclusion follows for any form of calibration parameter, and does so precisely because of the fundamentally low sensitivity of any probe to a change in static pressure close to M=1. It does not imply greater accuracy: the accuracy of a static-pressure probe calibration depends upon with which p is determined in the first place. However, the insensitivity to errors in true pressure, p, are much more immediately obvious for a calibration presented in the form I(M) than they are for p_d/p against M, for example.

The large effect of the probe body, evident in both the Disk-probe and pitch-probe calibrations, implies that measurements in flows with transverse variations of Mach number (or total pressure, or both) in the direction of the probe body are likely to be significantly in error. Measurements by the present author in a non-uniform flow were discarded for Mach numbers in excess of 0.8 because the implied streamline curvature was almost certainly spurious. Streamwise gradients of Mach number will affect the distance the shock stands ahead of the probe, and gradients large enough to cause a large change are also likely to cause significant errors.

7 ACKNOWLEDGEMENTS

The author is grateful to CERL for their permission to present this work at the Symposium.

8 REFERENCES

Bryer, D.W. & Pankhurst, R.C., 1971 Pressure-pobe methods for determining wind speed and flow direction. HMSO, London.

Chue, S.H., 1975 Pressure probes for fluid measurement. Prog. in Aerospace Sciences 16(2), 147-223.

Dudzinski, T.J. & Krause, L.N., 1969 Flow-direction measurements with fixed-postion probes. NASA TM X-1904.

Fransson, T.H., 1983 Aerodynamic probe calibrations. 7th Symp. "Measureing techniques in transonic and supersonic flows". Aachen.

Liepmann, H.W., & Roshko, A., 1966 Elements of gas dynamics. Wiley.

Shapiro, A.H., 1954 The dynamics and thermodynamics of compressible fluid flow, II. Ronald.

Wood, N.B. 1983 7th Symp. "Measuring techniques in transonic and supersonic flows". Aachen.

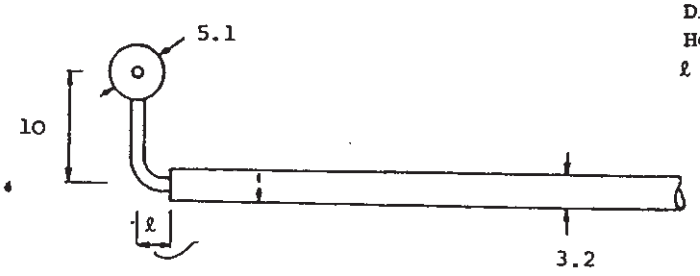

	DA	DB
Disk thickness	1.47	1.47
Hold diameter	0.80	0.80
ℓ	4	12

(a) Disk probes DA and DB (sensing hole passed through full thickness of both disks)

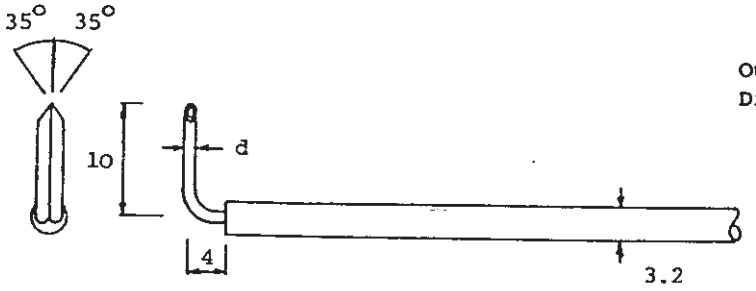

	YA	YB
Outside dia, d	1.24	1.07
Dia. ratio	0.63	0.67

(b) Yaw probes YA and YB

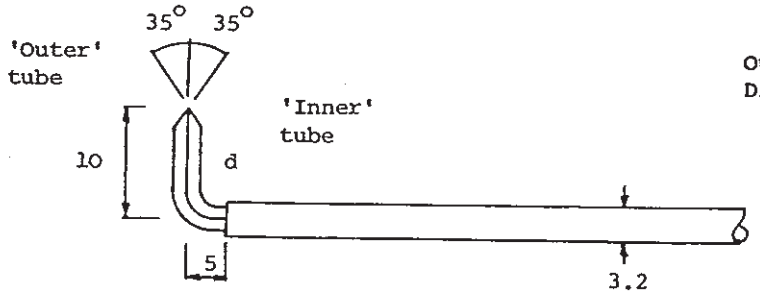

	PA	PB
Outside dia, d	1.24	1.07
Dia. ratio	0.63	0.67

(c) Pitch probes PA and PB

FIGURE 1 PROBE CONFIGURATIONS (Dimensions as mm.)

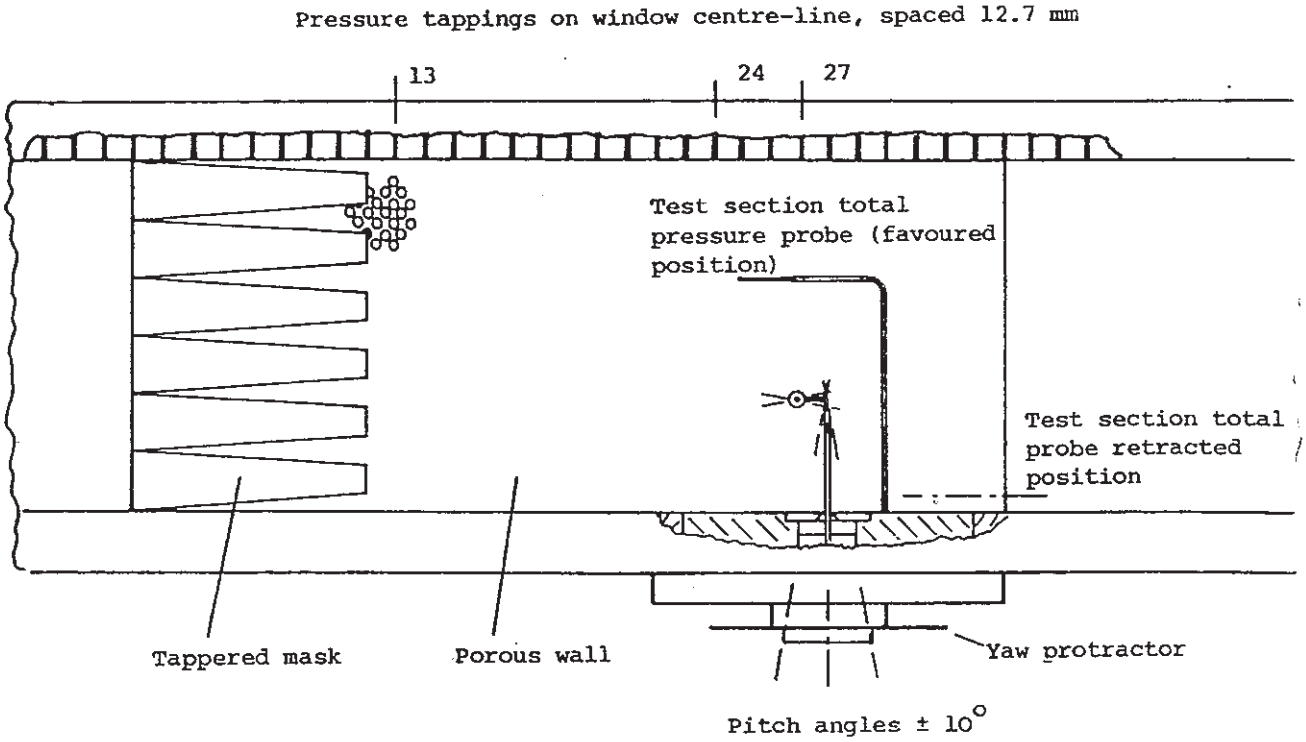

(a) Plan view

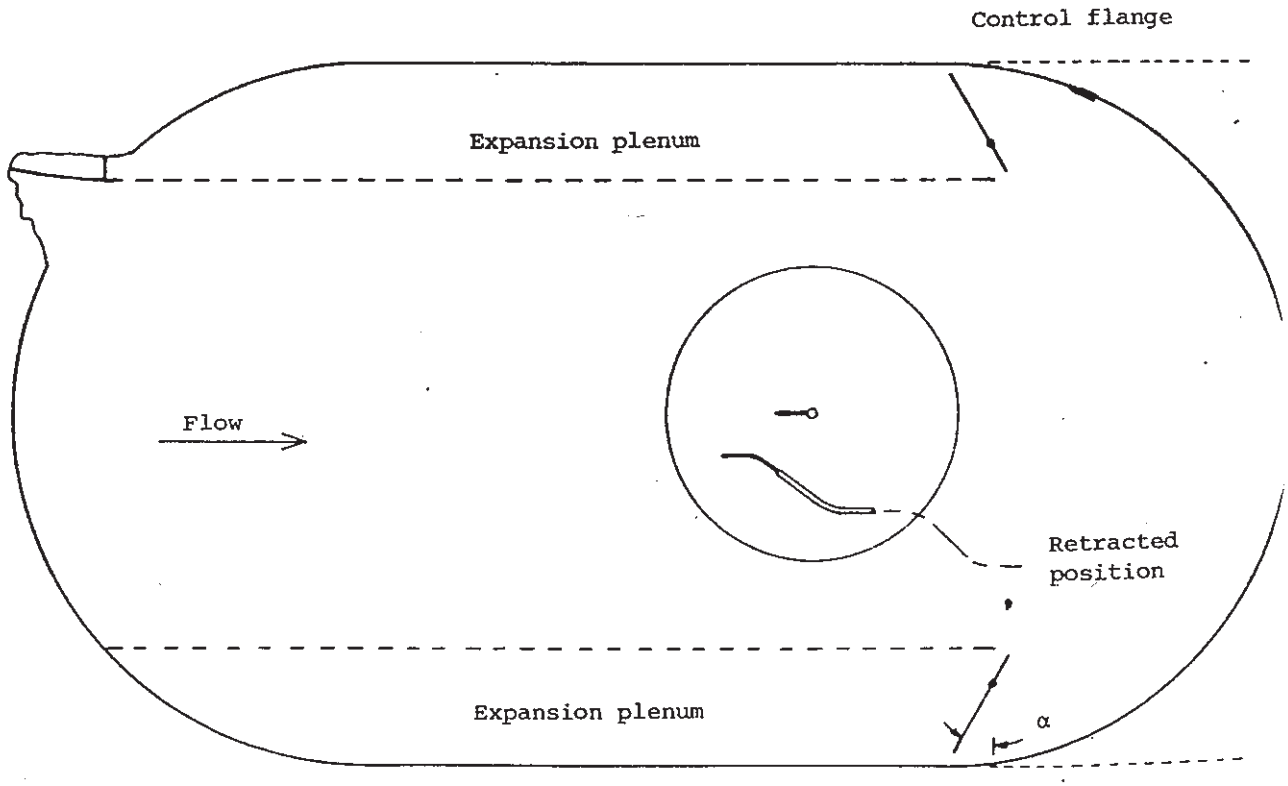

(b) Side elevation

FIGURE 2 TEST SECTION LAYOUT

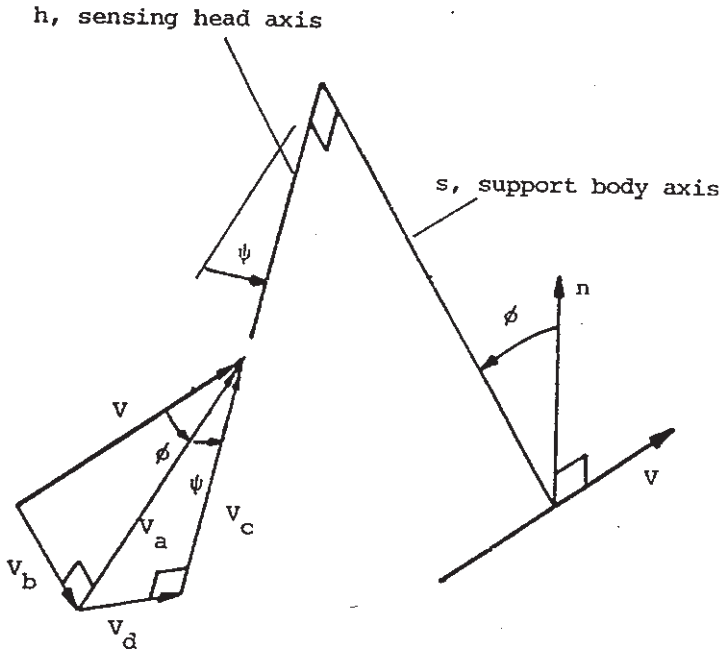

V	velocity vector	
s	Probe support axis	
n	Perpendicular to V in V-s plane	
ϕ	Angle between s and n	
h	Sensing head axis-perpendicular to s	
ψ	Rotation angle about s of h from V-s plant	
V_a	Vcos ϕ	in V-s plane
V_b	Vsin ϕ	in V-s plane
V_c	Vcos ϕ cos ψ	in h-direction
V_d	Vcos ϕ sin ψ	perpendicular to h-s plane

FIGURE 3 PITCH AND YAW ANGLE CONVENTION

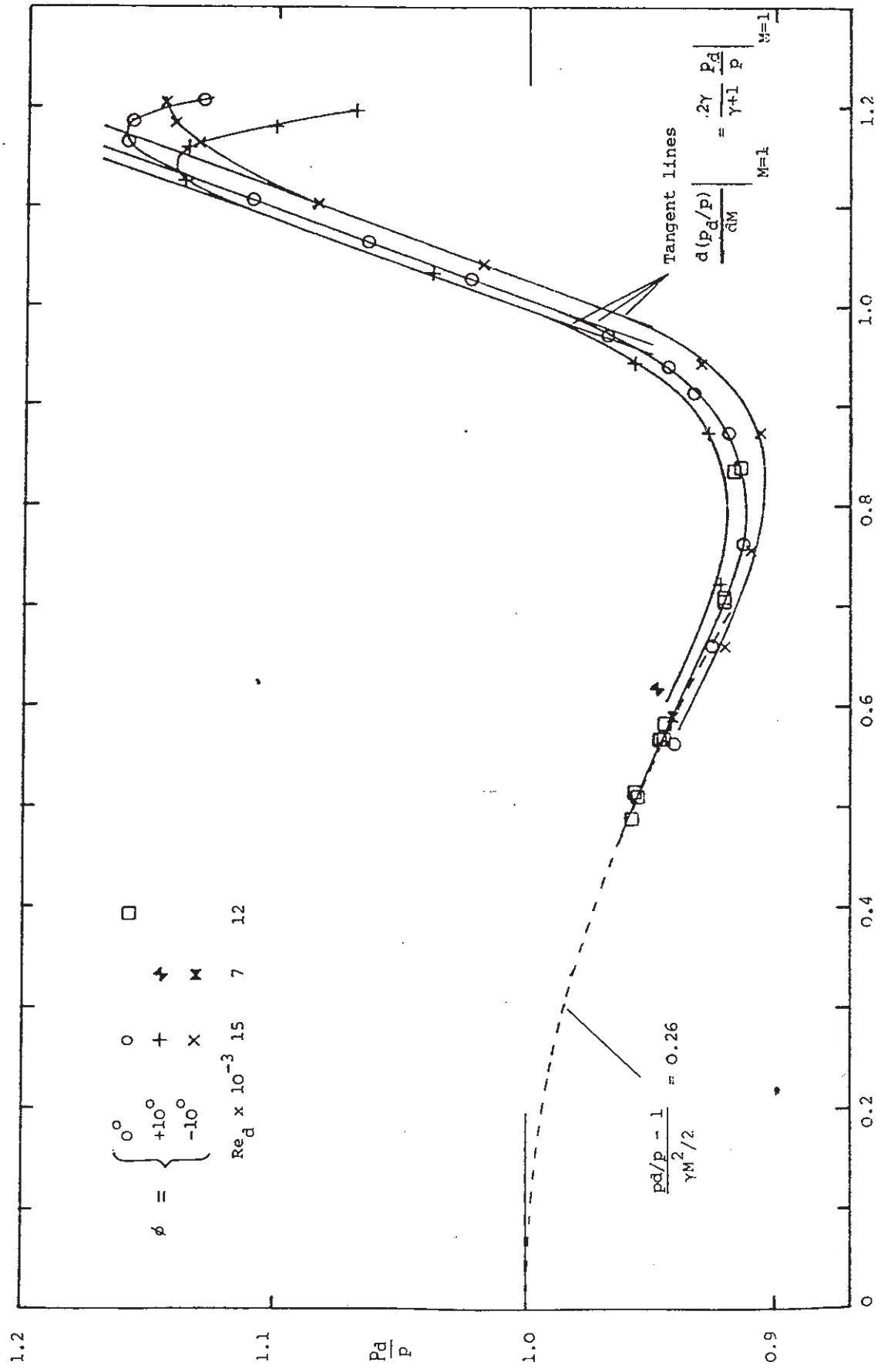

FIGURE 4 DISK PROBE DA CALIBRATION (Y = 0)

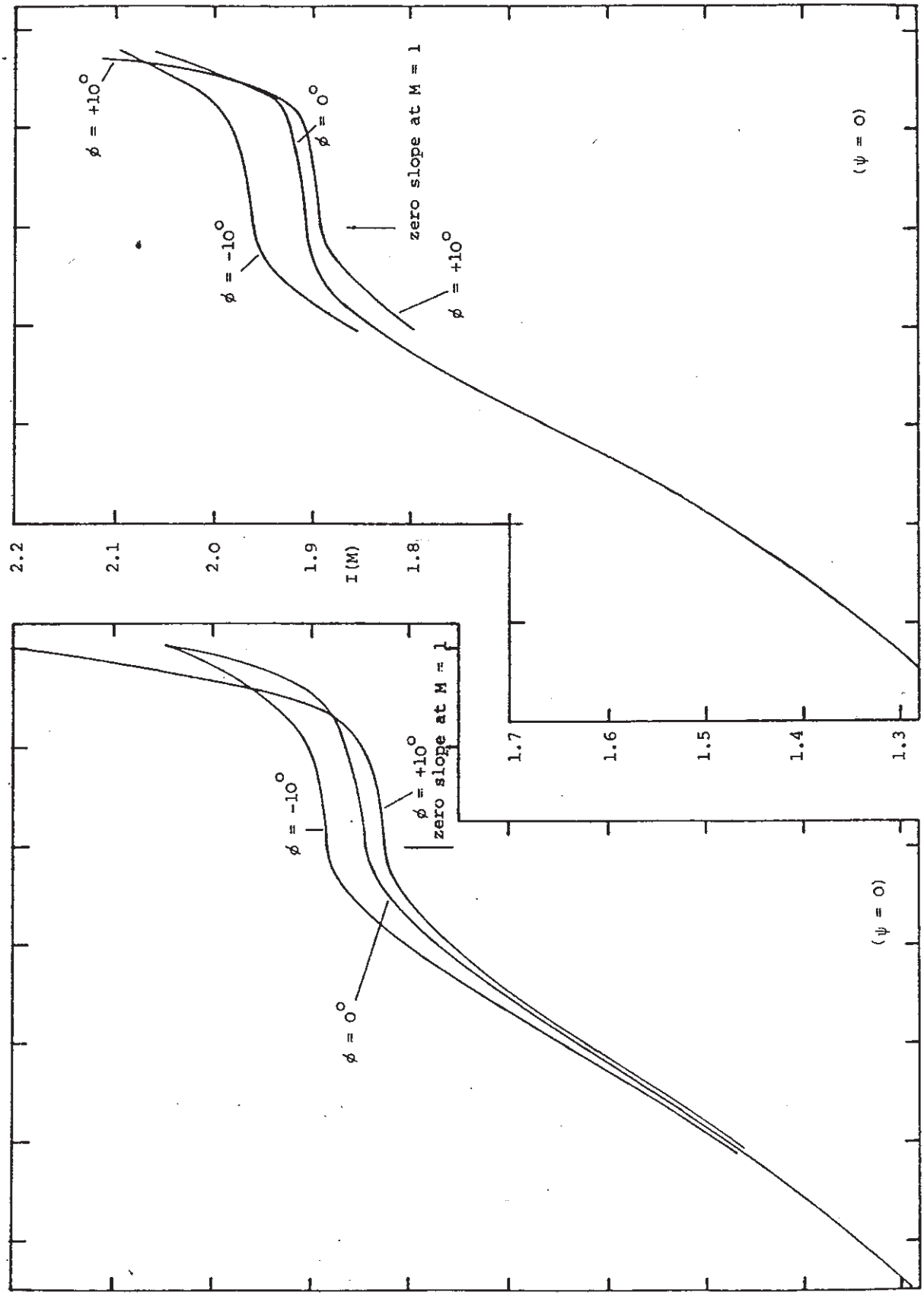

FIGURE 5 DISK PROBE DA INVERSION FUNCTION

FIGURE 6 DISK PROBE DB INVERSION FUNCTION

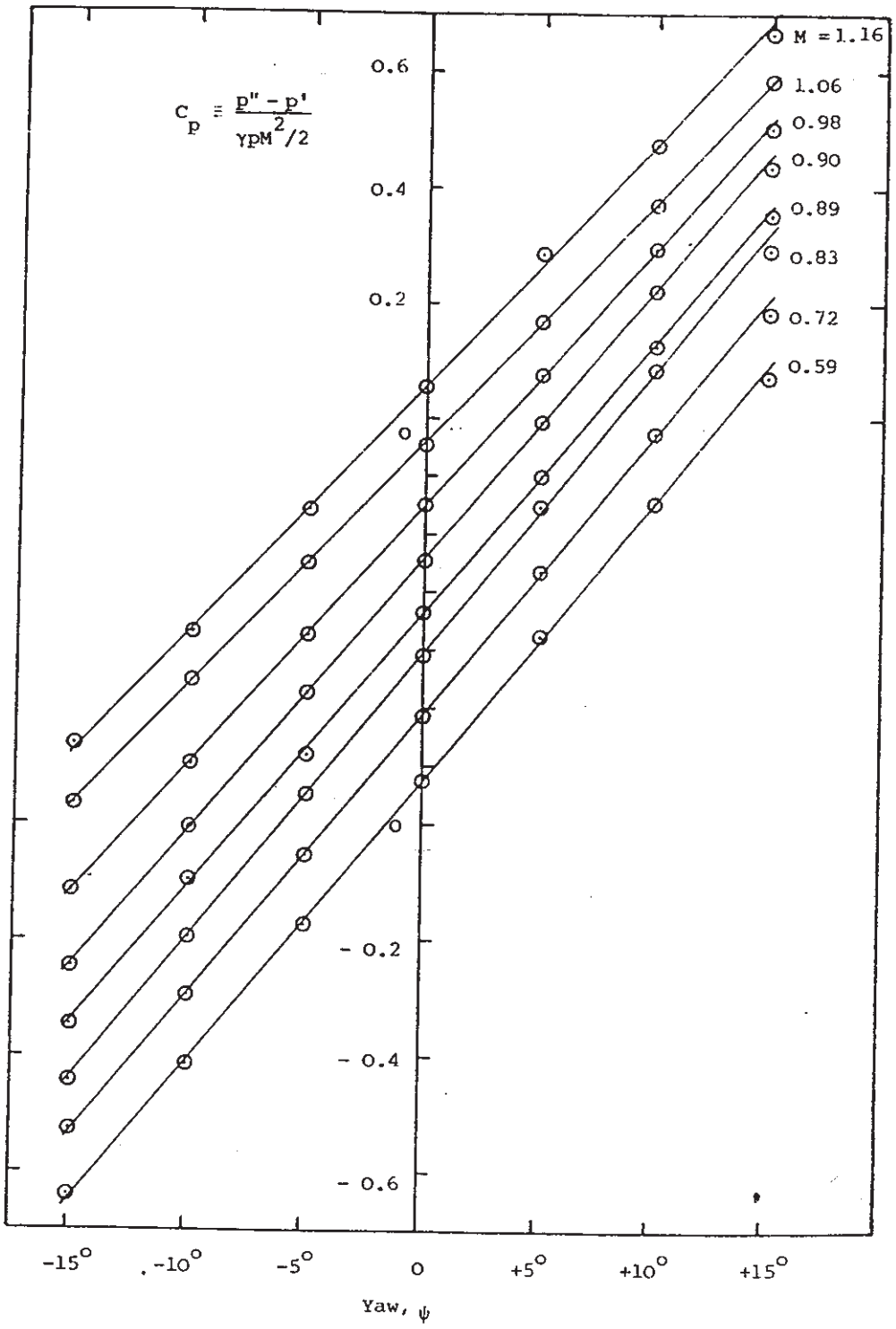

FIGURE 7 PRESSURE DIFFERENCE COEFFICIENT C_p OF YAW PROBE YA

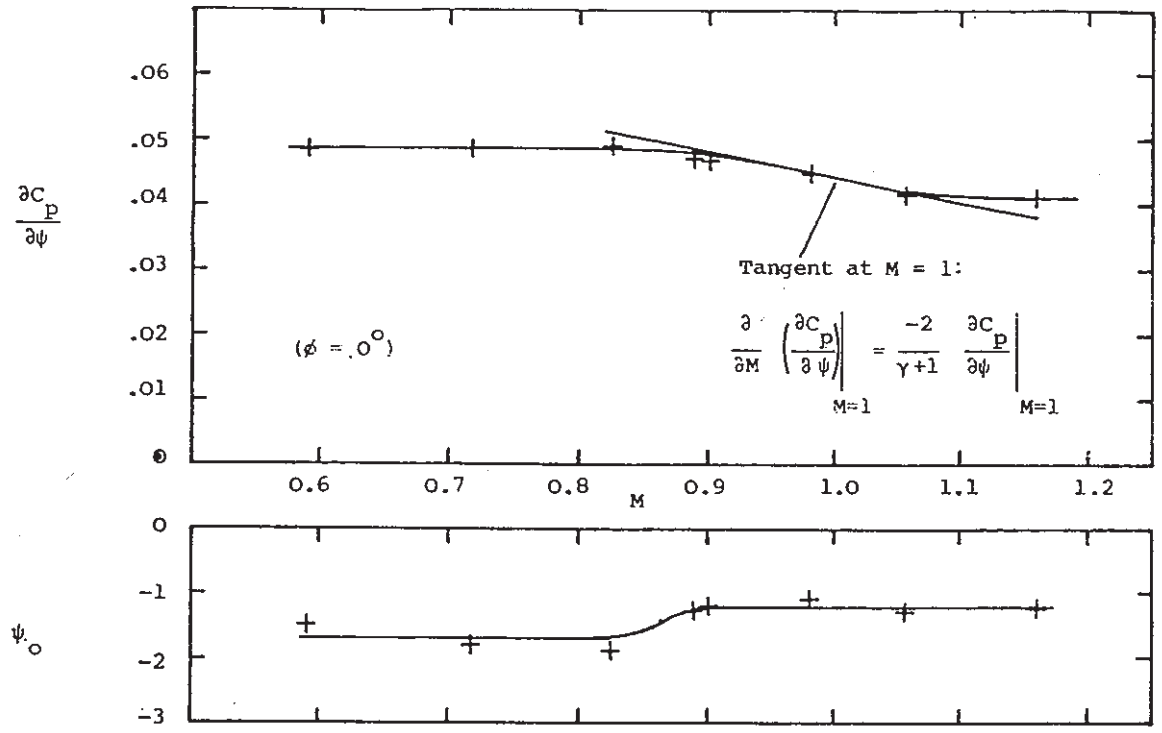

FIGURE 8 YAW PROBE YA CALIBRATION PARAMETERS

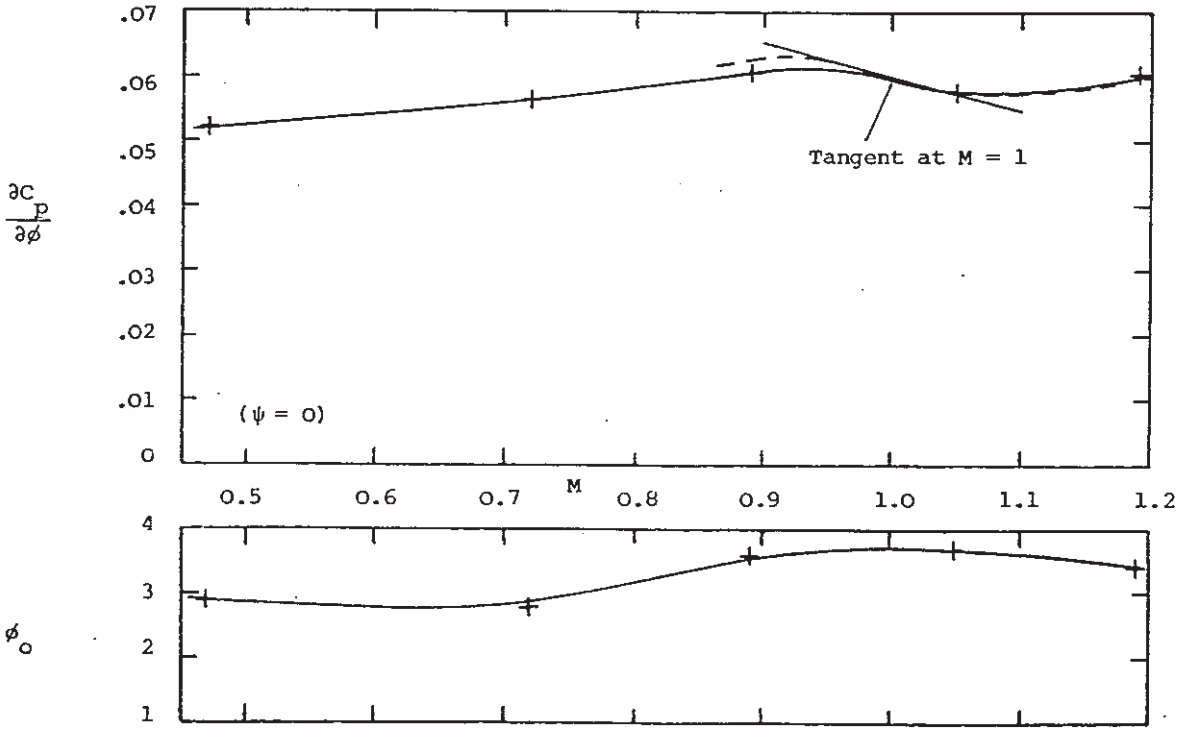

FIGURE 9 PITCH PROBE PB CALIBRATION (--- Pitch probe PA)

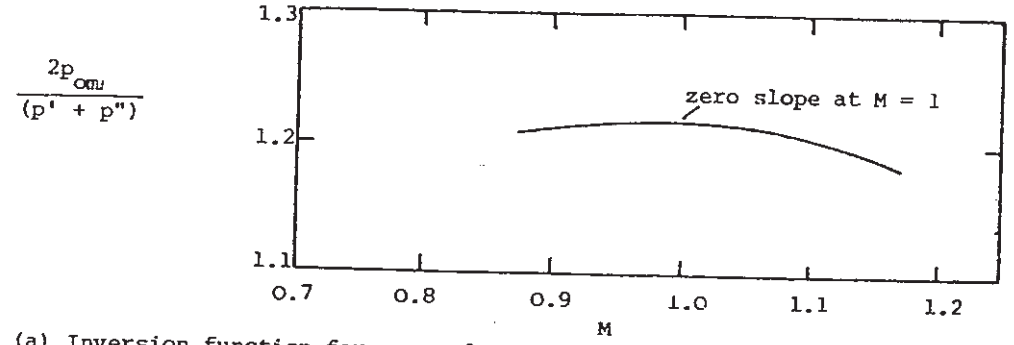

(a) Inversion function for yaw and total probes aligned with the flow

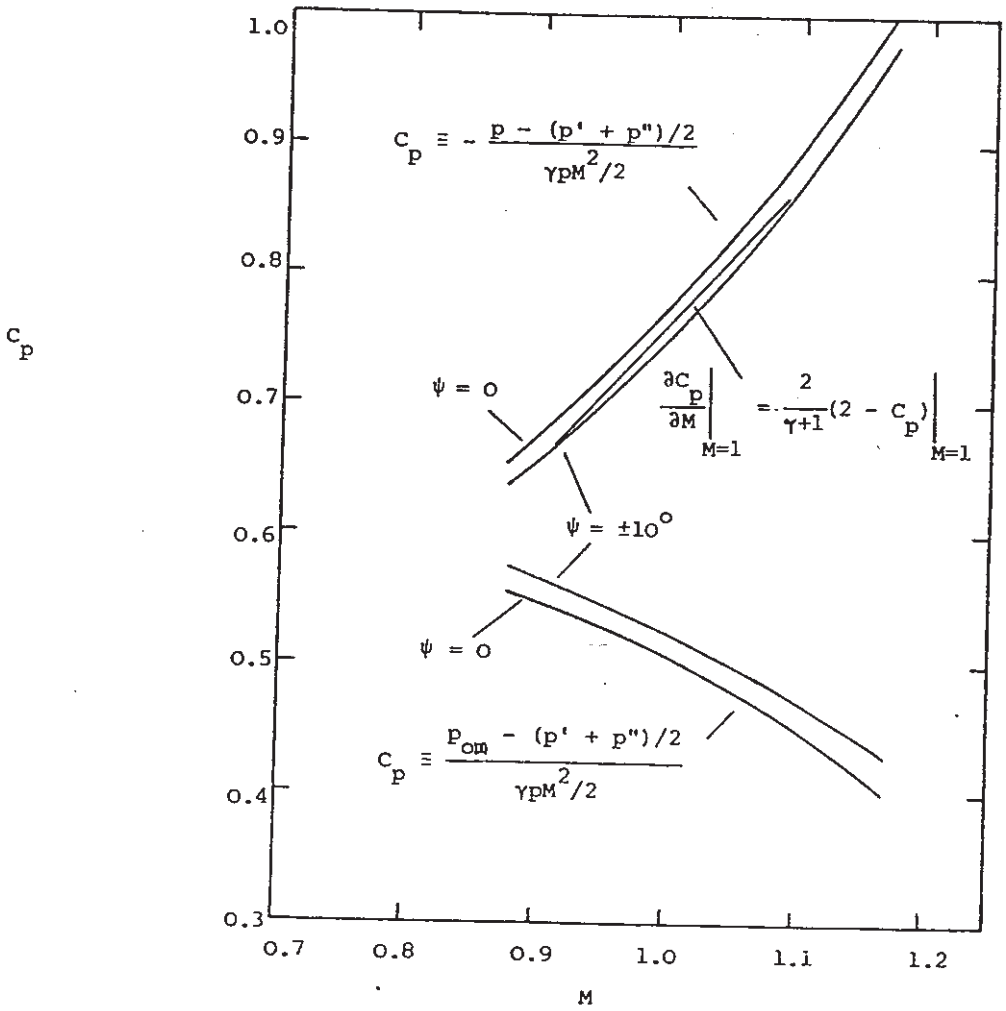

(b) Pressure coefficients for mean tube pressure $(p' + p'')/2$. C_p is defined in the Figure ($\phi = 0$)

FIGURE 10 PRESSURE RATIOS AND COEFFICIENTS FOR YAW PROBE YB

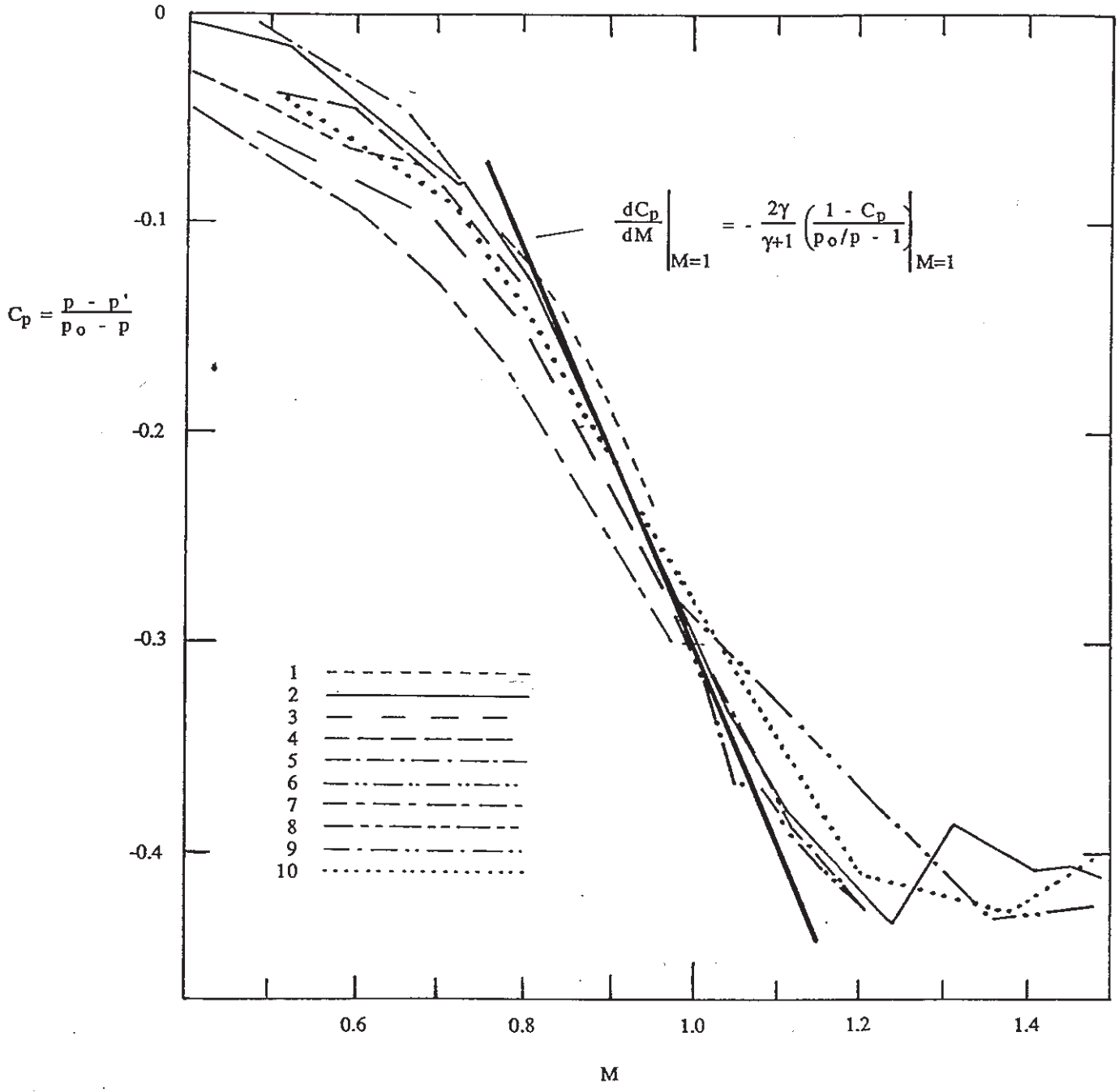

FIGURE 11 RESULTS FOR WP11 PROBE FROM 7th SYMPOSIUM.
1 - 20 are Institutes as defined at 7th Symposium.